NUEJ
Naresuan University
Engineering Journal

Effects of Stack and Heat Exchanger Configurations on Thermal Performance of a Thermoacoustic Refrigerator

W. Kamsanam[1*], R. Aungkurabrut[1] and F. Jinuntuya[1]

[1]Department of Mechanical Engineering, University of Phayao
*Corresponding author E-mail : tao_wasan@hotmail.com

(Received: January 15, 2018, Revised: June 18, 2018, Accepted: October 24, 2018)

Abstract

This paper discusses the influences of relevant parameters on thermal performance of a standing wave thermoacoustic refrigerator. The effects of the parameters, such as oscillating frequency, stack and heat exchanger configurations were investigated. The thermoacoustic refrigerator built for the current study comprised of a PVC resonator pipe of 1.05 metre in length and 2 inches of nominal diameter. A loudspeaker was installed at one end of the resonator pipe to oscillate the air, which was used as the working gas. Electrical power supplied to the loudspeaker was fixed at 42 W for the whole experiment. There were three set of stacks selected in this experiment; paralleled PVC sheet stacks of 3.5 cm and 10 cm long and aluminium wire mesh screen stack with a total length of 10 cm. Three heat exchangers were used; 2.0 cm and 22 cm long galvanized steel sheet heat exchanger and 2.0 cm long copper finned heat exchanger were included in the test. In the current study, the thermal performance of the refrigerator was represented in terms of air temperature at the cold end and hot end stack, room temperature and their differences. The results revealed that the resonant frequency was found at around 80 Hz. The system with aluminium wire mesh screen stack provided the best thermal performance comparing to paralleled plate stacks. The optimum stack position was at 70 cm measurement from the front of the loudspeaker. The lowest air temperature at the cold end stack was 7°C below the room temperature, which could contribute to the installation of the copper finned heat exchanger.

Keywords: thermoacoustic refrigerator, stack, heat exchanger.

1. NOMENCLATURE

B	blockage ratio
B_T	limit of error
b_T	systematic uncertainty
c_p	isobaric specific heat (J $kg^{-1}K^{-1}$)
D	gap spacing (m)
f	oscillating frequency (Hz)
K	specific heat ratio
k	thermal conductivity (W $m^{-1}K^{-1}$)
L	resonator length (m)
Ls	Stack length (cm)
l	half of plate thickness (m)
N	number of samples
R	gas constant (J $kg^{-1}K^{-1}$)
S	stack position (cm)
S_T	standard deviation
s_T	precision or random uncertainty
T	temperature (°C or K)
T_C	air temperature at cold end stack (°C)
T_H	air temperature at hot end stack (°C)
T_R	room temperature (°C)
U_T	overall uncertainty
v	speed of sound in gas (m s^{-1})
y_o	half of plate spacing (m)
δ_k	thermal penetration depth (m)
δ_v	viscous penetration depth (m)
λ	wave length (m)
μ	dynamic viscosity (N s m^{-2})
ρ	density (kg m^{-3})
ω	angular frequency (rad s^{-1})

2. INTRODUCTION

Nowadays, the global environmental problem has become an important issue to be considered. Greenhouse effect is one of the major concerns among the scientists. Refrigerants such as Chlorofluorocarbons (CFCs) and Hydrofluorocarbons (HCFCs and HFCs) are the examples of greenhouse gases. These gases significantly destroy the stratospheric ozone, and subsequently, enhance the greenhouse effect. Solutions for this situation may include producing alterative refrigerant gases such as Hydrofluoroolefin (HFO), CO_2, R290, R600 and R32 as well as developing new cooling process which is harmless to the environment. Thermoacoustic refrigeration is a state-of-the-art cooling system. It uses noble gases, for instance, Helium, Neon, Argon, Krypton, Xenon, air or their mixtures as the working fluid instead of the destructive refrigerants [1]. Such noble gases have low chemical reactivity and are transparent to the wavelengths of light which is responsible for trapping heat. Thus, these gases do not contribute to the greenhouse effects. It could be claimed that thermoacoustic devices are environment-friendly technology. In addition, the thermoacoustic refrigerator has less moving components compared to the vapor compression refrigerator. This is one of the main advantages in terms of reducing the maintenance cost. Thus, the thermoacoustic refrigeration could be a competitor of the traditional vapor compression system.

The main components of the thermoacoustic refrigerator are a resonator pipe, a linear driver or

loudspeaker which is used to generate acoustic waves, a stack and two heat exchangers. Once the gas parcels in the resonator pipe are oscillated because of the excitation from the driver, they experience compression and expansion causing a transport of heat from the lower to the higher temperature region. Besides the linear driver or loudspeaker, the thermoacoustic refrigerator can be driven by its reversed process device called thermoacoustic heat engine. Such refrigeration system would benefit communities in remote and rural areas of the developing countries. Saechan et al. [2] developed a thermoacoustic refrigerator driven by a combustion powered thermoacoustic engine. The refrigerator achieved the lowest temperature of -3.6^{o}C at the maximum coefficient of performance (COP) of 1.42 which was enough for cooling storage of crucial medicines. A similar apparatus was constructed by Jaworski & Mao [3]. The later setup provided better performance with the lowest temperature of -20.0^{o}C and the maximum achieved cooling load was 133W at the COP of 2.06. Apart from the biomass combustion, the waste heat from the exhaust gas of an internal combustion engine with high temperature of 700^{o}C could also be used as thermal input for thermoacoustic engine and refrigerator combination. This exploration had been revealed by Gardner & Howard [4]. According to their simulation results, the refrigerator would provide 135W cooling power and the temperature at cold heat exchanger would be -45^{o}C at its optimum operation. Nevertheless, the experimental data were not presented in the report. The comparison on COP of thermoacoustic refrigerator and vapor compression system was also modelled by Starr et al. [5]. They found that thermoacoustic refrigerator was suitable for low heat load application such as electronic devices cooling. However, for large heat loads, the COP of thermoacoustic refrigerator was less than the conventional vapor compression system.

There are many parameters that have significant influence on the performance of thermoacoustic devices. Tijani et al. [6] applied numerical approach for the optimization of different parts of thermoacoustic refrigerator. Tijani et al. [7] also performed an experimental investigation on the effects of gap spacing between parallel-plate stacks. The optimal spacing of about three times the thermal penetration depth was suggested. However, other geometries, such as length and position of stack were not mentioned in the report. The suitable design criteria for stack length, stack position and the gap spacing of stack and heat exchanger length established from computational method have been presented by Piccolo [8] and Nouh et al. [9]. Experimental studies related to the thermoacoustic refrigerator have also been done by other research groups. Assawamartbunlue & Kanjanawadee [10] presented experimental results of parameters such as stack position, plate spacing, stack length and thermal conductivity of stack which influenced the temperature profile on the stack. Actually, there was no heat exchanger installed at the stack extremities. A year later, Supperm et al. [11] added heat exchangers in a thermoacoustic refrigerator to observe thermoacoustic phenomenon. However, the effect of stack geometry on the refrigerator performance was not investigated. The effects of both stack parameters and heat exchanger were determine by Dhuchakallaya & Saechan [12]. The optimum geometry of stack was suggested. Nevertheless, it was found that the heat exchanger installed at hot end stack did not contribute to the temperature reduction on the cold end stack.

As the heat transfer process plays an important role on the overall performance of thermoacoustic devices, the fabrication technique for the heat exchanger in oscillatory flow condition was presented by Garrett et al. [13]. The convective heat transfer coefficient for oscillatory flow was predicted, but the influence of heat exchanger parameters on thermoacoustic refrigerator performance was not depicted. Basically, the heat transfer process in the oscillatory flow is quite complex. As pointed out by Nsofor et al. [14], the straight flow heat transfer correlation is not applicable for analyses of the thermoacoustic system. Thus, the design of the heat exchanger for the thermoacoustic device needs to be further investigated.

As reviewed earlier, the effects of stack configurations have been numerically examined in [6] and [8]. Considering the experimental works, stacks made from thin plastic sheet rolled into spiral pores were tested as mentioned in [10] and [12]. To satisfy the experimental requirements, the effects of stacks with different configurations are needed to be investigated. In [11] and [12], the setup of thermoacoustic refrigerators were equipped with heat exchangers. The enhancement of cooling performance because of the heat exchangers was not reported in [11]. In [12], there was no evidence to exhibit the advantage of hot heat exchanger on thermoacoustic refrigerator performance which differs from that stated in [13]. Thus, the investigation regarding this parameter is required to be performed.

In this study, the influence of oscillating frequency was carried out and the resonance frequency for the developed apparatus was determined. For the effects of stack configurations, parallel sheets stacks and an aluminium wire mesh screen stack were chosen for the current experiment. The optimum length and position of stack were also examined. As the hot heat exchanger might have impact on the thermoacoustic refrigerator operation, heat exchangers of different configurations were selected and their influences were be observed.

3. EXPERIMENTAL APPARATUS AND PROCEDURES

The thermoacoustic refrigerator developed for this experiment is of standing wave type. It composes of main components such as a resonator pipe, a stack, a hot heat exchanger and a loudspeaker within the enclosed box (Fig. 1). One heat exchanger is situated on the hot side of the stack. This heat exchanger is responsible for ejecting heat from the system. On the cold side of the stack, it is a vacant space to simulate no-heating load situation. Although the overall performance of thermoacoustic

device is influenced by the working gas [15, 16], this parameter is beyond the scope of the current study. Thus, the air at the atmospheric pressure is used as the working fluid for simplicity.

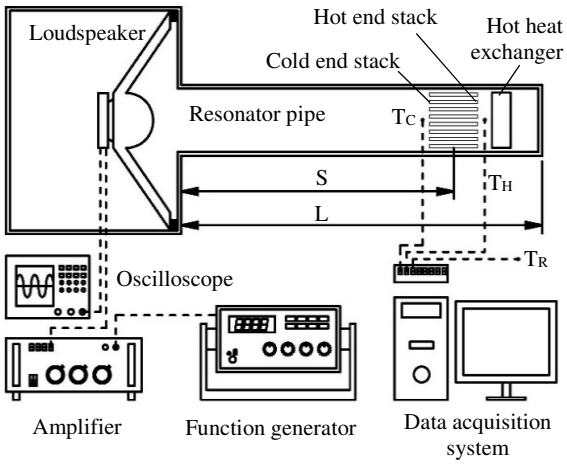

Figure 1 A schematic diagram of the standing wave thermoacoustic refrigerator in the current study.

The resonator is an essential component with other parts attached to it. For this reason, it must be strong enough and have rigid surface for the sake of acoustic wave reflection. The PVC pipe is selected such that it can withstand the mean and dynamic pressure generated from the loudspeaker. Regarding thermal property, PVC pipe has a low thermal conductivity (0.17 W/m·K) [17]. Therefore, the heat leakage through the pipe surface is low. Since a heat exchanger will be installed at the hot end stack, small pipe diameter may cause difficulty for the heat exchanger fabrication and installation. As mentioned in [15], the loss of the acoustic power is proportional to surface area of the resonator, thus a compact resonator pipe has less acoustic power dissipation. Hence, a PVC pipe of 2 inches diameter is suitable for this study. According to the specification of loudspeaker used in this study, its resonant frequency, which characterizes the highest excursion, is about 69 Hz. Referring to Equations (1) and (2) [18], a 1.05 m long resonator pipe is a compromise in this case considering that the length of the pipe (L) is twice the acoustic wave length (λ). In addition, this resonator length is applicable to install all the necessary components and is able to vary stack position for the investigation.

$$f = \frac{v}{\lambda} \quad (1)$$

$$v = \sqrt{KRT} \quad (2)$$

Another crucial component is stack. Basically, the stack in a standing wave thermoacoustic device is a pack of well-spaced thin solid sheets. Material of high heat capacity and low thermal conductivity is preferable. It is suggested that space between each plate of stack should be 2-4 times the thermal penetration depth (δ_k). The definition of δ_k can be seen in Equation (3) [19].

$$\delta_k = \sqrt{\frac{2k}{\rho c_p \omega}} \quad (3)$$

The thermal penetration depth is an important length scale in thermoacoustics. It represents a rough distance normal to the stack plate that the heat can diffuse through in a time interval of $1/\pi f$ [20]. If the stack is too dense, loss of the acoustic power because of the viscous effects will be prominent. Thus, viscous penetration depth (δ_v) as defined in Equation (4) [19] is another length scale in consideration.

$$\delta_v = \sqrt{\frac{2\mu}{\rho\omega}} \quad (4)$$

According to this experimental setup, the viscous penetration depth and thermal penetration depth is obtained at about 0.25 and 0.29 mm, respectively. Paralleled sheets stacks in this study are fabricated with gap spacing (D) of 1.0 mm corresponding to the recommended value; $2\delta_k < D < 4\delta_k$ (0.58 mm < D < 1.16 mm). Porosity or blockage ratio of stacks defined by Equation (5) is 0.77.

$$B = \frac{y_o}{y_o + l} \quad (5)$$

The length and the position of stack also have great influences. Three set of stacks, as detailed in Table 1, are included in the test. Stack No.1 and No.2 consist of parallel plates which is made from Polyvinylchloride (PVC) sheet. Stack No. 3 comprises of many pieces of aluminium mesh screen packed together to achieve a total length of 10 cm. Drawing of all stacks are depicted in Fig. 2.

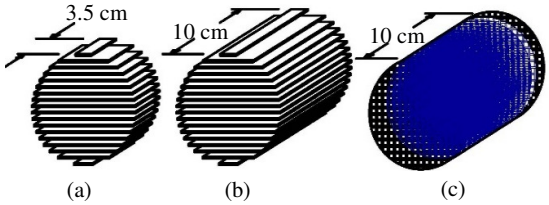

Figure 2 Illustration of stacks. (a) Stack No.1: 3.5 cm long paralleled sheets, (b) stack No.2: 10 cm long paralleled sheets and (c)stack No.3: 10 cm long wire mesh stack

Thermal interaction between the working gas and the solid surfaces is crucial for the performance of the thermoacoustic devices. It is assumed that the capability of heat removing from the system may determine the overall performance of the thermoacoustic devices. Thus, three heat exchangers of various configurations, as presented in Table 1, were developed to perform as a hot heat exchanger. HEX-1 and HEX-2 are of air cooling type. They are made of galvanized steel sheet curled into a hollow cylinder of the same diameter as the resonator pipe. HEX-3 is a copper finned type with water cooling. The fin length measured in gas flow direction was 2 cm while the fin thickness and gap spacing were 0.3 and 1.0

mm, respectively. The cooling water flows in a cavity on the housing circumference. Water at room temperature was used as a cooling medium and the flow rate was kept at 0.2 LPM. There is a small gap of about 5 mm between the hot end stack and HEX-3 in order to minimize the heat flowing back to the stack. Drawing of all heat exchangers is illustrated in Fig. 3.

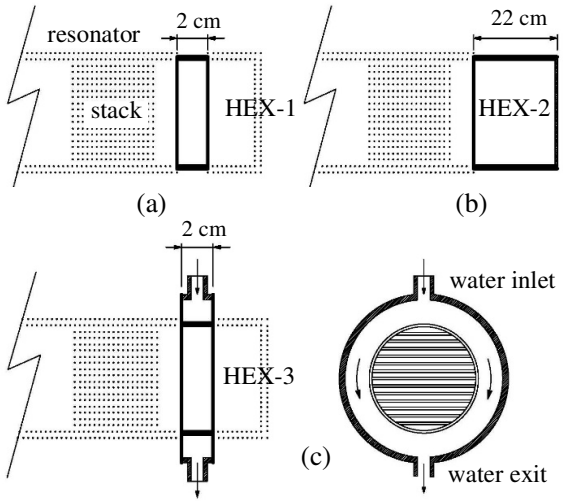

Figure 3 Illustration of HEX-1 (a), HEX-2 (b) and HEX-3 (c).

Table 1 Components of the thermoacoustic refrigerator

Components			
Resonator			
Material	PVC pipe		
Diameter	2" Nominal diameter		
Length	1.05 m		
Stacks	No. 1	No. 2	No. 3
Material	Paralleled PVC sheets	Paralleled PVC sheets	Aluminium wire mesh
k	0.19 W/m·K	0.19 W/m·K	222 W/m·K
c_p	1,470 J/kg·K	1,470 J/kg·K	940 J/kg·K
Length	3.5 cm	10 cm	10 cm
Gap spacing	1 mm	1 mm	-
Thickness	0.3 mm	0.3 mm	0.3 mm
Porosity	0.77	0.77	0.79
Hot Heat Exchanger (HEX)			
	HEX-1	HEX-2	HEX-3
Material	Galvanized steel sheet curled into a hollow cylinder		Copper fins
Length	2 cm	22 cm	2 cm
Cooling liquid	Air	Air	Water

The oscillation of the working gas was induced by an 8 inches loudspeaker. Sine wave signal from a function generator (YOKOGAWA-FC39) was provided through an audio amplifier to drive the loudspeaker at selected frequencies. Electrical power was fixed at 42 W which was less than a half of the loudspeaker rated power. At this level, displacement amplitude of the loudspeaker diaphragm will not exceed its maximum linear excursion of ±3.1 mm. This can avoid the damage of loudspeaker. In addition, operating at the mentioned level can minimize the drop of force factor which could result in the loss of the acoustic power and the dynamic pressure. However, to fully understand the influences of audio loudspeaker characteristic, a series of experiments are need to be further conducted. Regarding the measurement, temperature data was acquired by means of type T thermocouple probes and data acquisition system. The air temperature at the cold end stack (T_C), the hot end stack (T_H) and the room temperature (T_R) were collected. The thermocouple probes for measuring T_H and T_C are located at around 2 mm away from the stack extremities (Fig. 1). This location was selected to avoid direct thermal contact of the probes and stack surface. Additionally, the probes are also situated within travelling distance of gas parcels during the oscillation.

At first, the thermoacoustic phenomenon was observed. This was done on the experimental setup with stack No.1 situated at position S = 50 cm and no heat exchanger installed. The effect of oscillating frequency was examined by varying the driving frequency from the function generator. Once the system was in steady condition, thermoacoustic effect was noticed through the variation of T_C and T_H. Regarding the influences of position, the stack was moved to various positions: S = 20, 30, 70 and 90 cm. The optimum location was determined by the largest temperature difference between the room temperature and the cold side temperature ($T_R - T_C$). Thereafter, stack No.2 and No.3 was tested with the same procedure. When the optimal stack configuration was determined, each of HEX-1, 2 and 3 was installed consecutively to find the most suitable one. From the experiment, it was expected that a suitable stack and heat exchanger would be determined. Furthermore, it was assumed that the installation of the hot heat exchanger could result in the decrease of T_C.

Since the results in this study will be represented by T_R, T_C, T_H and their differences, the source of uncertainty mainly arises from temperature measurement. Basically, the uncertainty can be categorized into two groups: precision or random uncertainty (s_T) and systematic or fixed uncertainty (b_T) [21]. Precision uncertainty for the temperature measurement (s_T) can be calculated from Equation (6) [22]. According to a preliminary temperature measurement, the estimation of precision uncertainty for the temperature measurement (s_T) is ±0.17°C.

$$s_T = S_T / \sqrt{N} \qquad (6)$$

Regarding the systematic uncertainty of the temperature measurement (b_T), it cannot be directly determined by any statistical technique. However, it is obtained from the equipment specifications given by manufacturers and, then, estimated according to Equation (7) [23]. In the current experiment, temperature measurement was acquired by type T thermocouple (class 1 tolerance) which has limit of error (B_T) at 1.0°C. Hence, the systematic uncertainty of the temperature measurement (b_T) is ±0.5°C

$$b_T = B_T/2 \quad (7)$$

The overall uncertainty of the temperature measurement (U_T) can be estimated from Equation (8). Referring to the values of s_T and b_T obtained from Equations (6) and (7), the overall uncertainty evaluated at 95% confidence level was ±0.53°C.

$$U_T = \sqrt{s_T^2 + b_T^2} \quad (8)$$

4. EXPERIMENTAL RESULTS AND DISCUSSION

In this study, the thermal performance of standing wave thermoacoustic refrigerator is represented by air temperature at the hot end (T_H) and the cold end (T_C) of the stack comparing with the room temperature (T_R). The temperature information was selected to present here rather than the cooling capacity or the COP to minimize the uncertainty in the measurement. In a small cooling capacity system, if the temperatures are converted to COP, the uncertainty imbedded in the temperature measurement will propagate into the final results. Interpretation of the influences of the interested parameters on thermoacoustic refrigerator performance can be misleading. In addition, a basic setup of the test rig is designed in order to avoid any interference from additional components and measurement devices. Hence, at this stage, temperature data could be employed as a guideline in thermoacoustic refrigerator design procedure.

4.1 Thermoacoustic phenomenon with time evolution

In Fig. 4, air temperature T_H, T_R, T_C and T_R-T_C are illustrated. Temperature profiles were obtained from the setup with stack No.2 and S =50 cm without the heat exchanger while the oscillating frequency was kept at 70 Hz. The temperature measurement from all probes were validated with a calibrated sensor. Prior to run the loud speaker, the temperature data were acquired for several minutes in order to ascertain that all thermocouple probes provided comparable temperature values in the same environment. This can be seen from the temperature readings for the first five minutes in Fig. 4, which shows the values for the three probes are at about 22.5°C. Once the loudspeaker was excited at 5½ minutes, the air started to oscillate and thermoacoustic effect was observed when T_H increased and T_C decreased. The hot area of stack is located adjacent to the closed end of resonator pipe as the air experiences a compression at the pressure antinode during the oscillating cycle. This phenomenon is consistent with the experimental results reported in [11] and [12].

Temperature difference $T_R - T_C$ is presented by the bottom line shown in Fig. 4. It is noticed that $T_R - T_C$ continuously increases from around 0°C (at 5½ minutes) to 5°C (at 9 minutes) and keeps constant until 18 minutes. After that, $T_R - T_C$ shows a slight fall of about 0.5–1.0°C. Considering T_H, it kept rising since the loudspeaker was on. This occurrence might be because of the fact that the heat dissipation to the surrounding room was lower than that amount of heat being pumped from the cold end stack. This occurrence resulted in heat accumulation around the hot end stack. In such case, the thermal performance of the thermoacoustic refrigerator may get worse because air temperature at the cold end stack rises gradually after running the system for a certain time duration. According to this observation, it is supposed that if heat accumulation at the hot end stack could be diminished, the thermoacoustic refrigerator performance would be improved. For this reason, the significance of the hot heat exchanger installed next to the hot end stack has been taken into account and discussed thereafter

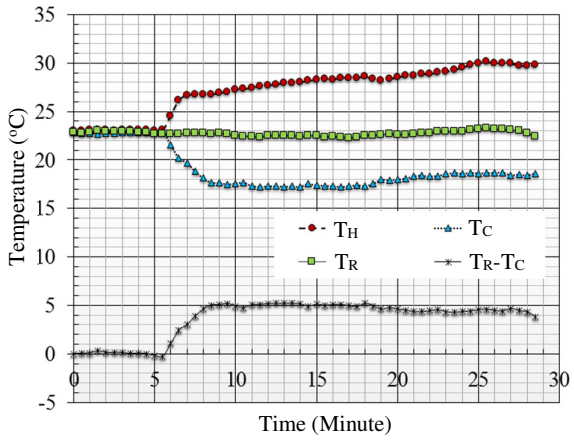

Figure 4 Temperature profiles from the setup with stack No.2, S =50 cm and operating at 70 Hz with no heat exchanger.

4.2 Oscillating Frequency

In Fig. 5, the oscillating frequency is varied from 30 Hz to 120 Hz with the increment of 1.0 Hz for every step. $T_R - T_C$ represents how cold is the air at the cold end stack comparing with the room temperature. $T_R - T_C$ profile shows upward trend from the oscillating frequency of 30 Hz and reaches the peak of about 4.6°C at 77 Hz, after which the drop has appeared. When oscillating frequency was adjusted closer to the resonant frequency, more intense compression applied on the gas parcels as they were traveling toward the pressure antinode. This situation caused the gas parcels to be hotter until achieving the highest temperature at the resonant frequency. According to Fig. 5, the air temperature at the hot end stack (T_H) as well as the difference of hot end and cold end temperature ($T_H - T_C$) reach the peak at 80 Hz. This point is considered as the resonant frequency of the current system. For frequencies beyond the resonance, both T_H and $T_H - T_C$ steadily decreased until the upper frequency limit in this experiment was attained.

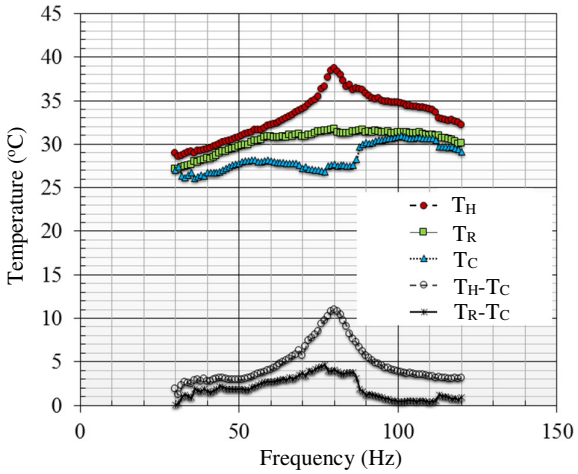

Figure 5 Air temperature vs. oscillating frequency of the setup with stack No.2 and S =50 cm with no heat exchanger.

4.3 Stack Configurations

The temperature profiles of $T_R - T_C$ for the setup with different stacks are presented in Fig. 6. It can be observed that at the frequency below 55 Hz and most frequency above 88 Hz, stack No.1 gives higher $T_R - T_C$ than that of stack No.2. However, the frequencies in those regions are quite far from the system resonance thus the cooling effect is small. Considering the temperature at or nearby the resonant frequency, $T_R - T_C$ for stack No.2 is higher than that of stack No.1. Basically, the stack functions as a medium for temporarily storing the heat while it is transported from the cold end to the hot end of it. The short stack like the stack No.1 may not be able to hold temperature gradient along the surface. In addition, the acoustic power dissipation because of the friction is another crucial parameter for a long stack. However, the tests for stacks longer than 10 cm were not performed in this study. This can be an essential issue for further investigation.

Regarding the material, the stack that has low thermal conductivity is preferable because heat conduction from the hot end to the cold end will deteriorate the cooling capacity of thermoacoustic refrigerator. Furthermore, material with high heat capacity is required in order to maintain the temperature gradient along the stack and to keep the local temperature on solid surface to be steady. As depicted in Fig. 6, stack No.3 which is made from aluminium wire mesh screen, shows the higher peak of $T_R - T_C$ than that of stack No.1 and No.2 made from paralleled PVC sheet. Once the thermal properties of the PVC sheet and the aluminium wire mesh screen are considered as detailed in Table 1, a substantially high thermal conductivity of the aluminium stack should have negative effect on $T_R - T_C$. This consequence could be because of the heat-transfer-resistant air layers between each piece of the mesh. Thus, heat conduction through the aluminium wire mesh screen stack would be diminished.

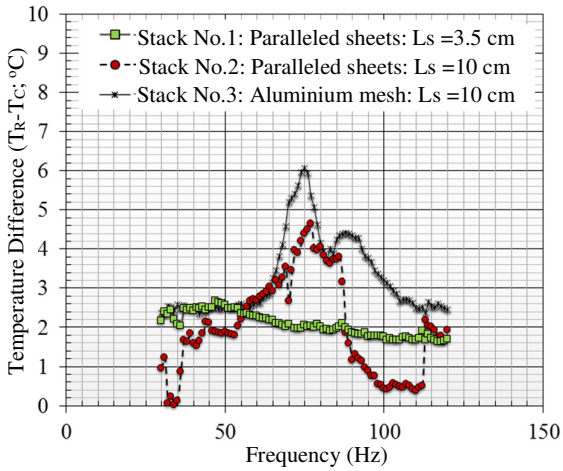

Figure 6 The influences of stack configurations on $T_R - T_C$ for the setup at stack location S =70 cm with no heat exchanger.

Stack position in the thermoacoustic refrigerator is also a key parameter having a great impact on the overall performance. In Fig. 7, the influences of stack position on $T_R - T_C$ for the setup of stack No.3 with no heat exchanger is presented. It can be observed that the stack which is located close to the loudspeaker (S = 20 cm) and the one which is placed nearby the close end of the resonator (S = 90 cm) do not reveal the peak of $T_R - T_C$. For the positions of stack at 50 and 70 cm, the peak of $T_R - T_C$ are about 5 and 6°C, respectively. Thus, it can be determined that the optimum position of the stack for this test rig is at S = 70 cm.

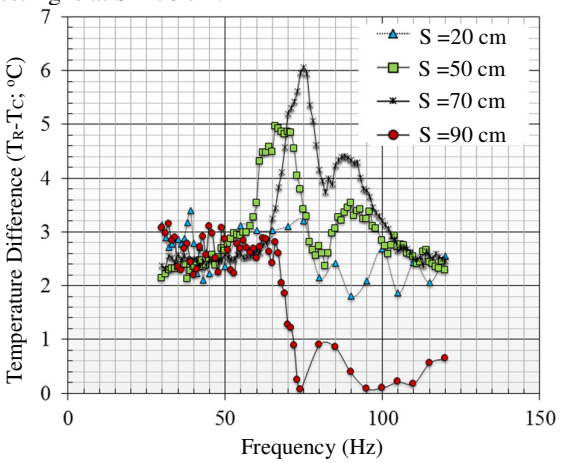

Figure 7 The influences of stack position on $T_R - T_C$ for the setup of stack No.3 with no heat exchanger.

According to Fig. 7, the higher the S, the closer is the stack to the closed end of resonator which is a velocity node. The gas velocity amplitude will be lower at the position closer to this end. Since the viscous dissipation loss is proportional to the square of the gas velocity amplitude, the decreasing of velocity amplitude will result in a reduction of the losses. Thus, the peak of $T_R - T_C$ for S = 70 cm is better than those for S = 20 and 50 cm. Nevertheless, the acoustic power proportions to the

imaginary part of the product of the pressure amplitude and the gas velocity amplitude. This implies that acoustic power will drop if stack is installed too close to the velocity node. This could be the explanation that the stack situated at S = 90 cm provides the worst $T_R - T_C$. Thus, a compromise on the stack positioning is also required.

4.4 Impact of the hot heat exchanger

To determine the influence of the heat transfer capability at the hot side of stack on the thermal performance of the thermoacoustic refrigerator, three types of heat exchangers were tested and compared with the original arrangement, i.e. without the heat exchanger. Fig. 8 shows that $T_R - T_C$ for HEX-1 and HEX-2 are similar and lower than that of the original setup. Basically, the resonator should be chosen from a rigid material so that it can effectively reflect the acoustic wave. In case of HEX-1 and HEX-2, which was made from the galvanized steel sheet, might not be strong enough for the working gas as a rigid boundary. As a result, $T_R - T_C$ got worse comparing with the original setup. For HEX-03, the peak of $T_R - T_C$ was higher than that of the original resonator pipe of about 1°C. However, it was found in [12] that T_C could not be further reduced by adding a hot heat exchanger. Their results might not be consistent with that obtained in this study; the discrepancy might be because of the difference in the heat exchangers' configuration. In [12], two heat exchangers were built for the test. They were made from spiral copper tube: one was a bare tube and another one was a bare tube attached by copper scourer to increase the heat transfer area. These two heat exchangers might have caused high pressure drop because of the blockage from the spiral tube, while HEX-3, in the current study, had less flow obstruction. Fig. 9 shows, the difference in $T_H - T_R$ is approximately 3°C between the peak of the original resonator (higher peak) and that of the setup with HEX-03 (lower peak). This indicates the impact of the heat exchanger in thermoacoustic devices.

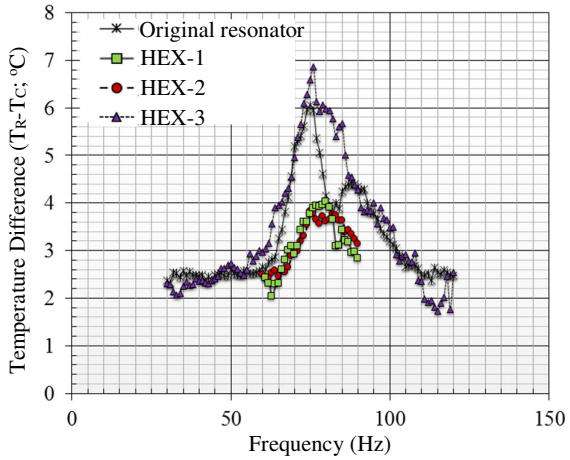

Figure 8 The influence of the hot heat exchanger on $T_R - T_C$ for the setup with stack No.3 at location S =70 cm.

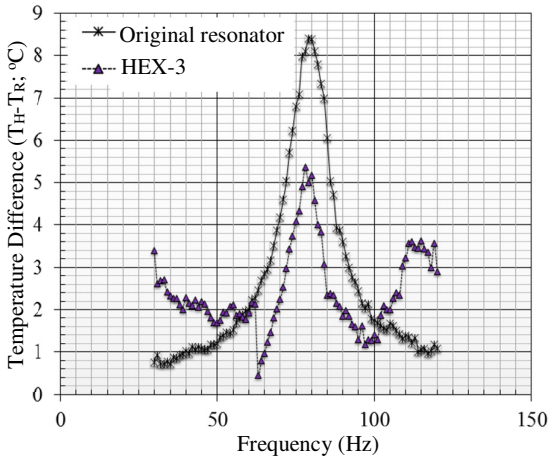

Figure 9 The influence of the hot heat exchanger on $T_H - T_R$ for the setup with stack No.3 at location S =70 cm.

5. CONCLUSION

In the near future, thermoacoustic refrigeration could be a potential competitor to vapor compression system because it has less moving parts and uses noble gas as the working fluid. However, the investigation on the effects of various parameters on the performance is required. In this study, the resonant frequency is found at around 80 Hz from the experimental setup. Regarding the stack configuration, the optimum position is at S = 70 cm. The stack material is also a crucial matter. Generally, a stack of high heat capacity and low thermal conductivity is required. It is found that stack No.3, which made from aluminium wire mesh screen, provides the largest $T_R - T_C$. This could be because of the heat-transfer-resistant air layers between each mesh screen. Since heat from the cold end stack will be transported and accumulated at the hot end stack, a hot heat exchanger could benefit the refrigerator performance. The suitable heat exchanger in this experiment is HEX-3, which is a water cooled copper finned heat exchanger. According to the results, the lowest air temperature measured at the cold end stack is obtained at around 7°C below the room temperature.

This study focuses on the thermal performance in terms of air temperature at the cold end and hot end stack comparing with room temperature. The results could be used as a guideline for designing thermoacoustic refrigerator. However, a system filled with compressed noble gas to achieve higher cooling capacity would be required for further investigation. Then, the experimental results could be presented in terms of COP or other quantities. Moreover, additional parameters in accordance with finned heat exchanger configuration, such as fin spacing, fin length, resonator pipe parameters and input acoustic wave should be taken into account.

6. ACKNOWLEDGEMENT

The authors gratefully acknowledge the contributions of Mr. Piyachat Anusornhirunkarn, Mr. Sutakorn Phosing, Mr. Arthit Deemee, Mr. Supawich Khemkhan

and Miss Rapeepun Tojing for their help in setting up a part of the experimental apparatus and a preliminary testing on the system capability. The authors also appreciate the useful comments and contributions of the reviewers and the editors.

7. REFERENCES

[1] Belcher, J. R., Slaton, W. V., Raspet, R., Bass, H. E., & Lightfoot, J. (1990). Working gases in thermoacoustic engines. Journal of the Acoustical Society of America, 105(5), 2677-2684.

[2] Saechan, P., Kang, H., Mao, X., & Jaworski, A. J. (2013). Thermoacoustic refrigerator driven by a combustion-powered thermoacoustic engine-demonstrator of device for rural areas of developing countries. In Lecture Notes in Engineering and Computer Science, World Congress on Engineering, London, UK, 3 - 5 July 2013, 2097-2102.

[3] Jaworski, A. J., & Mao, X. (2013). Development of thermoacoustic devices for power generation and refrigeration. In Proceedings of the Institution of Mechanical Engineers, Part A: Journal of Power and Energy, 227(7), 762-782.

[4] Gardner, D. L., & Howard, C. Q. (2009). Waste-heat-driven thermoacoustic engine and refrigerator. In Proceedings of Acoustics 2009, Adelaide, Australia, 23-25 November 2009,

[5] Starr, R., Bansal, P. K., Jones, R. W., & Mace, B. R. (1996). The reality of a small household thermoacoustic refrigerator. International Refrigeration and Air Conditioning Conference, Indianapolis, United States, 323-328.

[6] Tijani, M. E. H., Zeegers, J. C. H., & De Waele, A. T. A. M. (2002). Design of thermoacoustic refrigerators. Cryogenics, 42, 49-57.

[7] Tijani, M. E. H., Zeegers, J. C. H., & De Waele, A. T. A. M. (2002). The optimal stack spacing for thermoacoustic refrigeration. The Journal of the Acoustical Society of America, 112(1), 128-133.

[8] Piccolo, A. (2013). Optimization of thermoacoustic refrigerators using second law analysis. Applied Energy, 103, 358-367.

[9] Nouh, M. A., Arafa, N. M., & Abdel-Rahman, E. (2014). Stack parameters effect on the performance of anharmonic resonator thermoacoustic heat engine. Archive of Mechanical Engineering, 61(1), 115-127.

[10] Assawamartbunlue, K., & Kanjanawadee, P. (2009). Experimental demonstration of thermoacoustic cooling. Journal of Research in Engineering and Technology, 6(1), 1-24.

[11] Supperm, S., Jangsawang, W., & Mingmuang, N. (2010). Study of sound wave cooling. Srinakharinwirot University Journal of Science and Technology, 2, 106-114.

[12] Dhuchakallaya, I., & Saechan, P. (2015). Numerical and experimental study on the stack geometry affecting on the cooling performance of the thermoacoustic refrigerator. Journal of King Mongkut's University of Technology North Bangkok, 25(3), 381-392.

[13] Garrett, S. L., Perkins, D. K., & Gopinath, A. (1994). Thermoacoustic refrigerator heat exchangers: Design, analysis and fabrication. In Proceedings of the 10th International Heat Transfer Conference, Brighton, United Kingdom, 375-380.

[14] Nsofor, E. C., Celik, S., & Wang X. (2007). Experimental study on the heat transfer at the heat exchanger of the thermoacoustic refrigerating system. Applied Thermal Engineering, 27, 2435-2442.

[15] Swift, G.W. (1988). Thermoacoustic engines. Journal of the Acoustical Society of America, 84(4), 1145-1180.

[16] Tijani, M. E. H., Zeegers, J. C. H., & De Waele, A. T. A. M. (2002). Prandtl number and thermoacoustic refrigerators. The Journal of the Acoustical Society of America, 112(1), 134-143.

[17] Sekisui Chemical (2008). ESLON SCH80 PVC & CPVC Piping Systems Specifications & Engineering Manual (1st ed., 112). Tokyo, Japan: Sekisui Chemical.

[18] Çengel, Y. A., & Boles, M. A. (2007). Thermodynamics: An engineering approach (6th ed., pp. 855) Singapore: McGraw-Hill.

[19] Wheatley, J., Hofler, T., Swift, G. W., & Migliori, A. (1983). An intrinsically irreversible thermoacoustic heat engine. The Journal of the Acoustical Society of America, 74(1), 153-170.

[20] Swift, G.W. (1995). Thermoacoustic engines and refrigerators. Physics Today, 48(7), 22-28.

[21] Kim, J. H., Simon, T. W., & Viskanta, R. (1993). Journal of heat transfer policy on reporting uncertainties in experimental measurements and results. Journal of Heat Transfer, 115(1), 5-6.

[22] Miller, V. R. (2002). Recommended guide for determining and reporting uncertainties for balances and scales. US Department of Commerce, Technology Administration, National Institute of Standards and Technology.

[23] Dieck, R. H., Steele, W. G., & Osolsobe, G. (2005). Test Uncertainty. ASME PTC 19.1-2005. New York: American Society of Mechanical Engineers.

8. BIOGRAPHIES

Dr. Wasan Kamsanam received his PhD in Mechanical Engineering (2014) from the University of Leicester, UK. Currently he is a lecturer at the University of Phayao, Thailand. His research interest includes heat transfer phenomena in oscillatory flow and thermoacoustic technology.

Dr. Rachaneewan Aungkurabrut received her PhD in Aerospace and Mechanical Engineering (2011) from University Of Texas at Arlington, USA. She is currently a lecturer at the University of Phayao, Thailand. Her research interest includes Micro and capillary reactor technology; biodiedel; Fischer-Tropsch process.

Dr. Fontip Jinuntuya received her PhD in Aeronautical and Automotive Engineering (2015) from Loughborough University, UK. She is currently a lecturer at the University of Phayao, Thailand. Her research interest includes proton exchange membrane fuel cell and lattice Boltzmann modelling.